ISSN impresa 0717-3644
ISSN online 0718-221X

Maderas. Ciencia y tecnología 16(4): 435 - 444, 2014

DOI:10.4067/S0718-221X2014005000035

PREDICTING THE YOUNG'S MODULUS OF DEFECT FREE RADIATA PINE SHOOKS IN FINGER-JOINTING USING RESONANCE FREQUENCY

How S.S [1], C.J Williamson[1,♠], D Carradine[2], Y.E Tan[3], J Cambridge[4], S Pang[1]

ABSTRACT

In this paper, dynamic MOE and static MOE of short-length radiata pine specimens produced for finger jointing were measured using non-destructive technique and correlated to each other. In order to obtain reliable static MOE data, 36 mm thickness shooks as well as the matched samples of reduced thickness (15mm) were tested, and the effect of annual growth rings on dynamic and static MOE is also addressed. Mathematical correlations were fitted between the dynamic MOE for the 36 mm thick shooks and the static MOE of the 15 mm thick samples. The coefficient of determination for dynamic MOE group 4,00-7,99 GPa was the strongest (R^2 = 0,82) and the correlation strength was further improved for sorted quarter sawn samples (R^2 = 0,92). Finally, the correlation between static modulus of rupture (MOR) and dynamic MOE is discussed.

Keywords: Dynamic MOE, static MOE, finger-jointing, radiata pine, non-destructive tool, modelling, shooks.

INTRODUCTION

In the last two decades, non-destructive testing (NDT) technique has been widely used in wood industry for mechanical property evaluation. The major advantage of the NDT technique is that the physical and mechanical properties of a material are quantified without altering its end-use capability (Ross and Pellerin 1994). The NDT technique includes visual and mechanical grading of wood, and application of electromagnetic radiation and sound waves. Non-destructive testing using acoustic and vibration methods was firstly introduced in 1945 (Hearmon 1945). After many years of development and improvements, the acoustic and vibration techniques are commonly used in forestry and wood industries at present, ranging from property measurements for standing trees (Brashaw *et al.* 2009, Ross and Pellerin 1994), logs (Ouis 1999), timber grading, and testing of laminated products (Bender *et al.* 1990, Nakai *et al.* 1989).

The determination of dynamic and static elasticity of a specimen is based on thin-plate theory. Both dynamic (Han *et al.* 1999) and static (Beer *et al.* 2009) elasticity theories were developed using the Euler-Bernoulli beam theory. In the development of NDT techniques, it is assumed that the test member is homogeneous and has the shape of a thin-plate or slender bar for a ratio of length-to-depth that is high enough so that the influence of transverse shear stress within the tested member is negligible. This length-to-depth ratio corresponds to the ratio of Young's modulus to shear modulus of the specimen (Kubojima *et al.* 2004). In practical applications, a pre-set threshold value is recommended in different standards for the length-to-depth ratio.

[1] Department of Chemical and Process Engineering, University of Canterbury, Christchurch, New Zealand.
[2] Structural Engineer, BRANZ Ltd., Porirua City, Wellington, New Zealand.
[3] Program Director, Forest Research Institute Malaysia (FRIM), Selangor D.E., Malaysia.
[4] Department of Mechanical Engineering, University of Canterbury, Christchurch, New Zealand.
♠ Corresponding Author: Vivian.how@pg.canterbury.ac.nz
Received: 14.04. 2013. Accepted: 04. 01. 2014.

In ASTM D198-05 (ASTM 2005), it is recommended that a structural member under three-point loading should have span-depth ratios between 11 and 15 while ASTM D143-94 (ASTM 2007) recommends that small clear specimens have a span-to-depth ratio of 14. Other standards such as the Japanese standard suggest that the span-to-depth ratio ranges from 15 to 19 for bending stiffness specimens and from 12 to 16 for bending strength specimens (JIS 1994).

Similar recommendations are also made for specimens for resonance testing, however, with different criterion. In the case of flexural resonance testing, the thickness of specimens should not be larger than one-sixth of the bending wavelength (Ljunggren 1991).

In the finger-jointing process, a piece of full length timber is cut into several short-length and defect-free sections known as "shooks", then finger-like profiles are made on the cut surfaces and finally these profiled shooks are glued into desired lengths known as finger-jointed timber. The thickness and width of the shooks are usually maintained to be the same as in the original timber but the shook lengths are between 150 and 500 mm after removing sections with defects. A report has suggested that shook length should not be greater than 400 mm to avoid jointing defects resulting from distortion (Satchell *et al.* 2010). However, shook with length close to 150 mm may not meet the required length-to-depth ratios recommended in testing standards.

Therefore, determination of mechanical properties of short shooks using appropriate techniques is important to optimise the overall property of the finger-jointed timber.

Correlations between dynamic modulus of elasticity MOE and static properties are commonly available in literatures which can be used to predict one property from the other measured ones (Wang 1998, Ilic 2001). However, these studies were conducted on specimens with dimensions that complied with length-to-depth ratios recommended in most standards. Therefore, there is a knowledge gap required to determine the mechanical properties of short length shooks from measurements using NDT techniques.

The objectives of the study were

- To develop regression functions that correlate the dynamic MOE based on flexural vibration and conventional static bending MOE for specimens of 15 mm thick and 36 mm thick, respectively.
- To assess the developed correlations by comparing and identifying the statistical significance in the regression relationships developed.
- To assess the effect of sawing pattern on the relationship between dynamic and static MOE.
- To assess if there is significant correlation between MOE and modulus of rupture (MOR) of the same specimen.

Maderas. Ciencia y tecnología 16(4): 435 - 444, 2014

MATERIALS AND METHODS

New Zealand radiata pine (*Pinus radiata*) samples with nominal dimensions of 120 mm x 36 mm x 290 mm, which are the typical dimensions in the New Zealand finger-jointing industry, were provided by a local finger-jointing company for experimentation. Seventy samples were carefully selected and divided into three groups based on sawing patterns, namely flat sawn (45 pieces), quarter sawn (12 pieces) and semi-sawn (17 pieces) as shown in Figure 1. The sawing pattern was firstly sorted on visual examination based on the overall growth ring orientation over the cross-section and then quantified by using Olson's method (Olson 1986).

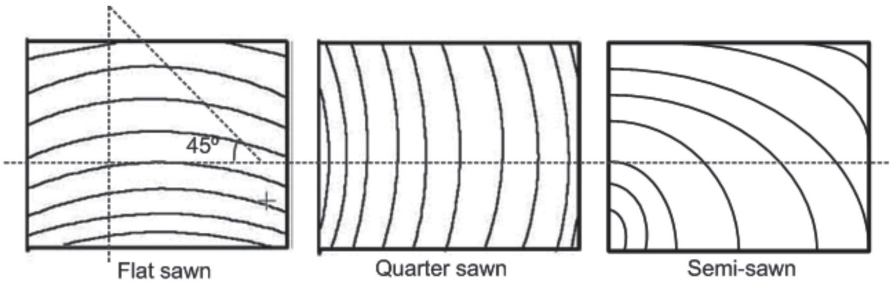

Figure 1. Determination of sawing pattern according to growth ring orientation on the end-grain section.

In Olson's method (1986), the growth ring orientation of a sample's cross section was measured by running a 45° triangle across the horizontal axis which had been marked prior to the measurement as shown in Figure 1. All of the growth rings were divided into two categories, i.e. greater than 45° and less than 45°. If a sample cross section had more than 70% area covered by growth rings with angle less than 45°, the sample was regarded as flat sawn. Similarly, if a sample cross section had more than 70% area covered with growth rings with angle greater than 45°, then the sample was classified as quarter sawn. The remaining samples having cross section covered with more than 30% of combination of sawn type were regarded as semi-sawn (Figure 1). Before test, dry density of each sample was measured which was found to range between 350 kg/m^3 and 550 kg/m^3, with most samples falling in the range of 400 kg/m3 and 530 kg/m^3. Then all samples were conditioned to targeted 12% moisture content.

Dynamic flexural MOE, static bending MOE, and static bending MOR

The experiments were conducted in the subsequent procedures:

- Dynamic MOE (E_{dyn}) and static MOE (E_{stat}) were measured for the 36 mm thick samples. This was to establish correlations between the dynamic MOE and the static MOE.
- Then all of the 36 mm thick samples were planed to 15 mm which were further tested for dynamic MOE, static MOE and static MOR. With reduction in thickness, the depth-to-length ratios of the samples were increased thus the results were expected to be improved. The results were used to assess the reliability of the test results of the 36mm samples.

In the static tests, the samples were loaded using the four-point static bending test machine following the procedure described in ASTM D198-05a (ASTM 2005). A 'U' shaped yoke deflectometer was placed on both edges of the test sample at the loading positions with a linear potentiometer being attached to the yoke to measure displacement at the neutral axis between the shear-free span of the sample. Loading speed was set at a constant rate of 1,0 mm/minute. The static MOE was calculated using the shear corrected Δ_{LB} equation (ASTM 2005).

In dynamic tests, samples were suspended on a bubble wrapped support system during measurement of resonance frequency. The supports were wrapped by using bubble wrap to simulate a free boundary condition as closely as possible.

A Brüel & Kjœr Handheld 2260 Investigator Fast-Fourier Transform (FFT) analyser was used to measure and compute the frequency. A Deltatron® piezoelectric accelerometer weighing 4,8 g was used as a sensor to pick up the magnitude of the resonance frequencies. The FFT analyser was set with a full scale of 3,270 ms^{-2}. The test configuration was set according to the first harmonic nodes in a free-free boundary condition as given in Harris (1988).

In this research, the natural frequency of flexural waves was measured. Dynamic MOE was calculated using the following equation which was initially proposed by Hearmon (1966):

$$E = \frac{0{,}946 f_F^{\,2} l^4 \rho}{d^2} \qquad (1)$$

After the dynamic tests and the static MOE tests, the 15 mm thick samples were loaded to rupture in the four-point static testing machine to determine MOR based on methods proposed in AS/NZS4063.1:2010 (1992). Relationships between the corresponding dynamic and static MOE with the MOR values were assessed.

RESULTS AND DISCUSSIONS

Comparison of results between E_{dyn36} and E_{stat15}

Statistical analyses were conducted using Z-test at alpha levels of 0,05 and 0,10 respectively, to assess the significant difference in the means between E_{dyn36} vs. E_{stat15} and the difference in the means between E_{dyn15} vs. E_{stat15}. The Z and P values as given in Table 1 indicate that the null hypothesis could not be rejected and that the difference in means of E_{dyn36} vs. E_{stat15} and in those between E_{dyn15} vs. E_{stat15} were statistically insignificant. Therefore, the correlation between dynamic MOE for 36 mm thick specimens and static MOE for planed 15 mm thick specimens was considered to be valid, suggesting the dynamic MOE can be used to determine the static MOE.

Table 1. Results from Z-Test for correlations of E_{dyn36} vs. E_{stat15} and E_{dyn15} vs. E_{stat15} at alpha level 0,05 and 0,10 respectively.

	Alpha level 0,05		**Alpha level 0,10**	
	E_{dyn36} vs. E_{stat15}	**E_{dyn15} vs. E_{stat15}**	**E_{dyn36} vs. E_{stat15}**	**E_{dyn15} vs. E_{stat15}**
Mean	1,0664	0,8261	1,0664	0,8261
Z value	1,0402			
Z critical two-tail	1,9600		1,6449	
P-value	0,2982		0,2982	

Correlations between E_{stat} and E_{dyn}

To establish correlations between Estat and Edyn, the experimental data and the predicted results are firstly assessed as shown in Table 2 with all of the samples being divided into five categories (Groups A to E) based on nominal E_{dyn36} values. However, the values presented in Table 2 did not take into account the effect of sawing pattern. The difference between E_{dyn36} and E_{stat15} and the difference between E_{dyn15} and E_{stat15} were computed to identify the discrepancies between dynamic stiffness and the corresponding static stiffness.

Table 2. Experimental data of E_{dyn36}, E_{dyn15}, E_{stat15} and maximum differences relative to E_{stat15} in various categories based on nominal E_{dyn36}.

Categories based on nominal E_{dyn36} (GPa)	Measured MOE values based on measured E_{dyn36} (GPa)			Maximum MOE differences based on data sorted by E_{dyn36} (GPa)	
	E_{dyn36}	E_{dyn15}	E_{stat15}	E_{dyn15} vs. E_{stat15}	E_{dyn36} vs. E_{stat15}
A: 4,0-6,0	4,81 - 5 ,99	4,77 – 6,85	4,03 – 6,74	(-)0,92 – (+)0,81	(-)0,83 – (+)0,78
B: 6,1-7,0	6,32 – 6,80	6,44 – 7,69	6,18 – 8,75	(-)1,60 – (+)0,69	(-)1,95 – (+)0,16
C: 7,1-8,0	7,10 - 7,99	7,33 – 9,55	7,40 – 10,79	(-)2,58 – (+)1,40	(-)3,10 – (-)0,02
D: 8,1-9,0	8,07 - 8,99	7,08 – 10,70	7,83 – 12,52	(-)3,23 – (+)0,58	(-)4,33 – (+)1,17
E: 9,1-11,0	9,78 – 10,98	8,50 – 10,17	9,37 – 14,27	(-)4,10 – (-)0,10	(-)3,71 – (+)1,33

From Table 2, it is found that when the data was sorted into different categories based on the nominal E_{dyn36}, correlation strengths were different for each category. In order to assess the reliability of the measured dynamic MOE, two correlations should be fitted, namely E_{stat15} vs. E_{dyn36} and E_{stat15} vs. E_{dyn15}. When all data were compiled and correlated without taking into the effect of sawing pattern, the linear-regression correlations have been fitted as shown in figure 2 with R^2 value of 0,73 for E_{stat15} vs. E_{dyn36} and 0,80 for E_{dyn15} vs. E_{stat15}, respectively.

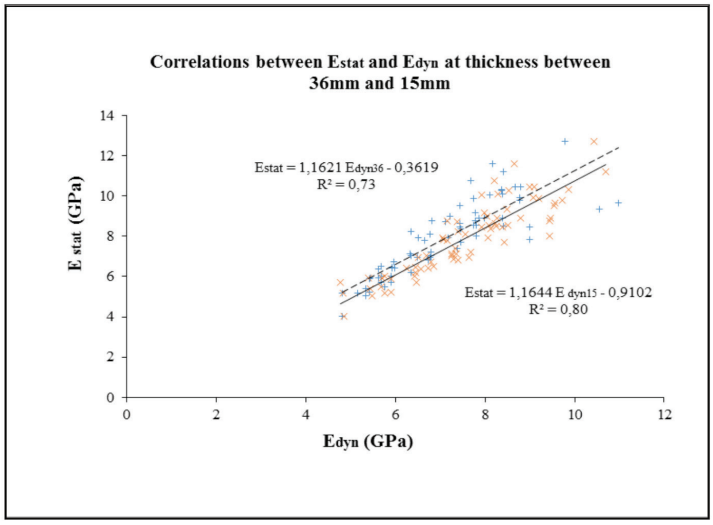

Figure 2. Linear regressions for correlations of E_{stat15} vs. E_{dyn36} and E_{stat15} vs. E_{dyn15}.

Figure 2 shows that the data are generally closely related; however, the significant data scattering from the regression lines has been observed for E_{dyn} ranging from 7 to 9 GPa. Verification on the predictability of the trend lines was explored using stepwise grouping on E_{dyn} and the results are given in Table 3, in which the data was regrouped based on nominal E_{dyn36} from the lowest value of 4 GPa to a different upper limit values.

Table 3. Assessment of significance in correlations between E_{stat} and E_{dyn} with stepwise grouping of data based on nominal E_{dyn36} from the lowest value of 4 GPa to different upper limit values.

Assigned dynamic MOE group (GPa)	Sort by E_{dyn36}		Sort by E_{dyn15}	
	No. of samples	R^2	No. of Samples	R^2
I : 4,00- 5,99	20	0,66	12	0,20
II : 4,00- 6,99	35	0,74	23	0,62
III : 4,00- 7,99	53	0,82	41	0,73
IV : 4,00- 8,99	67	0,79	58	0,78
V : 4,00-10,99	70	0,73	70	0,80

From Table 3, it is found that with regrouping of MOE, correlation strength for E_{stat15} vs. E_{dyn} was slightly improved for categories II, III and IV. The highest correlation strength was found in Group III with R^2 value of 0,82. However, the correlation for E_{stat15} vs. E_{dyn15} is worsened for other categories (Group I to IV) in comparison with the results in Figure 2. For practical applications, the following correlation is proposed to predict the static MOE based on the measured dynamic MOE for the 36 mm thick shooks used for finger-jointing timber:

$$E_{stat} = 0{,}57E_{dyn36}+2{,}45 \quad (2)$$

The above correlation is fitted for the static MOE values between 4 and 8 GPa, however, the correlation can be interpolated up to 11 GPa with slight reduction in R^2 (from 0,82 to 0,73).

In general, E_{stat15} were slightly higher by approximately 11% compared to E_{dyn36} and 6% higher than E_{dyn15}. The difference was consistent with findings by Haines *et al.* (1996) who compared the measured MOE values using flexural resonance with static MOE. It was found that the flexural resonance was merely 1 to 2% higher as compared to the corresponding static flexural MOE. Considering that different FFT analysers giving different resolutions to the frequency readings, the discrepancy in the present study (6 – 11%) is considered within acceptable experimental error.

Effect of Sawing Pattern on the Relationship between E_{dyn} and E_{stat}

The correlation between E_{stat} and E_{dyn} may be further improved by taking into account the effect of sawing pattern. Table 4 shows the linear regression coefficient of determination (R^2) for the relationship between E_{stat15} and E_{dyn36} and between E_{stat15} and E_{dyn15}, respectively, on samples with different sawing patterns.

Table 4. Linear regression coefficient of determination (R^2) for the relationship between E_{stat15} and E_{dyn} with consideration of sawing patterns.

Sawing Pattern	Coefficient of Determination (R^2)	
	E_{stat15} vs.E_{dyn36}	E_{stat15} vs. E_{dyn15}
Quarter sawn	0,92	0,86
Flat sawn	0,71	0,77
Semi-sawn	0,71	0,79

From Table 4, it is observed that the highest coefficient of determination (R^2) was achieved for quarter sawn samples. As for flat sawn and semi sawn samples, the correlation between E_{stat15} and E_{dyn15} was more significant than that between E_{stat15} and E_{dyn36}. The improvements in general are moderate by comparing the R^2 values listed in Table 3 and those given in Table 4. Although sawing pattern improves the correlations, the practical application may be problematic as it is difficult to sort the samples based on end-face growth rings in a finger-joint timber mill.

Relationship among Dynamic MOE, Static MOR and Wood Density

From the experimental data, the relationships among dynamic MOE, static MOR and wood density have been examined using multiple linear regressions and the results are presented in Table 5. In general, MOR has poor correlation of determination with the dynamic MOE and the wood density (R^2 = 0,11-0,14). The correlations of determination found from the present study are weaker than those reported in literature. For example, Jiang *et al.* (2007) measured dynamic MOE using the ultrasonic technique and correlated with MOR with R^2 values ranging from 0,16 to 0,41. In another study, the correlation of determination between ultimate tensile strength and dynamic MOE measured using longitudinal resonance was found to be between 0,24 and 0,74 (Ayarkwa *et al.* 2000). Olsson *et al.* (2010) correlated the static MOR with dynamic MOE measured on axial and transverse modes with R^2 values of 0,35 and 0,42, respectively. The weaker correlation of static MOR with dynamic MOE and wood density as found in the present study can be due to the sawing pattern and the sample thickness. The surface feature of the 15 mm samples is important in the MOR measurements. For a flat sawn sample, when the early wood band appeared on a sample surface, the measured MOR of the sample is expected to be reduced significantly. However for the quarter sawn samples, the sample surface usually contained a number of latewood and early wood bands, thus the effect of wood type (early wood and latewood) is much less compared to the flat sawn sample. This will be further examined in future study.

Table 5. Correlation significance for relationships among static MOR, static MOE, dynamic MOE, and wood density using multiple regression analysis.

Predictor	*Regressand*	R^2	*Level of significance at 95% confidence level*
Static MOE	$Edyn_{15}$ + density	0,79	***
Static MOE	$Edyn_{15,}$+ MOR	0,79	***
Static MOE	$Edyn_{15}$ + MOR + density	0,79	***
Static MOE	MOR + density	0,14	**
MOR	$Edyn_{15}$	0,11	**
MOR	$Edyn_{15}$ and density	0,14	**

CONCLUSIONS

Linear regression correlation between static MOE and dynamic MOE has been established for radiata pine shooks for finger-jointing timber manufacturing which can be used to predict the shook static MOE from measured dynamic MOE. The R^2 of the established correlation is 0,82 for measured dynamic MOE from 4 to 8 GPa and it is slightly reduced to 0,79 when the dynamic MOE upper limit is increased to 9 GPa. The R^2 value is further reduced to 0,73 when the dynamic MOE upper limit is 11 GPa. The correlation was developed from experimental data using 36 mm thick samples for dynamic MOE measurement and matched 15 mm thick samples for static MOE measurements. Statistical analysis has been performed in this study and the results show that this correlation can be used for other dimensions normally used in finger-jointing mill. The influence of sawing pattern on the correlation strength was also examined, however, significant improvement was only found in quarter sawn shooks. The proposed correlation will be used in future experimentation for estimating static MOE in developing a computer simulation system for finger-jointing processing.

Multiple linear regressions were performed to examine the correlations among static MOR, static MOE, dynamic MOE and wood density. The results show that the correlation strength between MOR and other parameters are poor. Further work will be performed to examine if the sawing pattern has significant influence on the static MOR.

REFERENCES

AS/NZS. 1992. Timber - Stress-graded - In-grade Strength and Stiffness Evaluation AS/NZS 4063-1992.

ASTM International. ASTM. 2005. Standard Test Methods of Static Tests of Lumber in Structural Sizes. D198-05a United States.

ASTM International. ASTM. 2007. Standard Test Methods for Small Clear Specimens of Timber. ASTM D143-94 (Reapproved 2007). West Conshohocken, United States.

Ayarkwa, J.; Hirashima, Y.; Sasaki, Y. 2000. Predicting tensile properties of finger-jointed tropical African hardwoods using longitudinal vibration method. *Ghana Journal of Forestry* 9: 45-56.

Beer, F.P.; ERJ, Jr.; DeWolf, J.T.; Mazurek, D.F. 2009. *Mechanics of materials* (5th Edition ed.). New York. McGraw-Hill.

Bender, D.A.; Burk, A.G.; Taylor, S.E.; Hooper, J.A. 1990. Predicting localized MOE and tensile strenght in solid and finger-jointed laminating lumber using longitudinal stress waves. *Forest Products Journal* 40(3): 45-47.

Brashaw, B.K.; Bucur, V.; Divos, F.; Goncalves, R.; Lu, J.; Meder, R.; Pellerin, R.F.; Potter,S.; Ross, R.J.; Wang, X.; Yin, Y. 2009. Nondestructive Testing and Evaluation of wood: A worldwide research update. *Forest Products Journal* 59(3): 7-14.

Haines, D.W.; Leban, J.M.; Herbe, C. 1996. Determination of Young's modulus for spruce, fir and isotropic materials by the resonance flexure method with comparisons to static flexure and other dynamic methods. *Wood Science and Technology* 30: 253-263.

Han, S.M.; Benaroya, H.; Wei, T. 1999. Dynamics of transversely vibrating beams using four engineering theories. *Journal of Sound and Vibration* 225(5): 935-988.

Harris C.M. 1988. *Shock and vibration handbook* (3rd ed.). New York. McGraw-Hill Co.

Hearmon, F.S. 1945. The fundamental frequency of vibration of rectangular wood and plywood plates. *Proceedings of Physical Society* 58(1): 78-92.

Hearmon, R.F.S. 1966. Theory of the vibration testing of wood. *Forest Products Journal* 16(8):29-40.

Ilic, J. 2001. Relationship among the dynamic and static elastic properties of air-dry Eucalyptus delegatensis R. Baker. *Holz als Roh- and Wekstoff* 59:169-175.

Jiang, J.H.; Lu, J.X.; Ren, H.Q.; Long, C.; Luo, X.Q. 2007. Assessment of flexural properties of different grade dimension lumber by ultrasonic technique. *Journal of Forestry Research* 18(4): 305-308.

Japan Standards Association. JSA. 1994. Methods of Tests for Woods. JIS Z2101-94

Kubojima, Y.; Ohtani, T.; Yoshihara, H. 2004. Effect of shear deflection on bending properties of compressed wood. *Wood and Fiber Science* 36(2): 210-215.

Ljunggren, S. 1991. Airborne sound insulation of thick walls. *Journal of Acoustic Society of America* 89(5): 2338-2345.

Nakai, T.; Tanaka, T.; Naao, H. 1989. Fundamental vibration frequency as a parameter for grading sawn timber. *International council for building research studies and documentation working commission W18A-Timber structures Berlin: Meeting* 22.

Olson, J.R. 1986. Measurement of growth ring orientation. Technical Notes. *Forest Products Journal* 36(3): 23-24.

Olsson, A.M.J.; Oscarsson, J.; Johansson, B.M.; Kallsner, B. 2010. Dynamic excitation and higher bending models for prediction of timber bending strength. *Paper presented at the The Future of Quality Control for Wood and Wood Products - The Final Conference of COST Action E53, Edinburgh. 4-7th May 2010.*

Ouis, D. 1999. Vibrational and acoustical experiments on logs of Spruce. *Wood Science and Technology* 33: 151-184.

Ross, R.J.; Pellerin, R.F. 1994. Nondestructive Testing for Assessing Wood Members in Structures - A Review. *Forest Products Report. Vol. FPL-GTR-70. Madison: FPL.*

Satchell, D.; Turner, J. 2010. Solid Timber Recovery and Economics of Short-rotation Small-diameter Eucalypt Forestry Using Novel Sawmilling Strategy Applied to Eucalyptus regnans. Theme: Diversified Species: Sustainable Forest Solutions & SCION. Report Number: FFR-DS028.

Wang, S.Y. 1998. Dynamic modulus of elasticity and bending properties of large beams of Taiwan-grown Japanese cedar from different plantation spacing sites. *Journal of Wood Science* 44: 62-68.

NOMENCLATURE

E or MOE	:	Young's Modulus (Pa)
MOR	:	Modulus of Rupture (Pa)
f_F	:	the 1st mode of flexural frequency (Hz)
l	:	length of specimen (m)
d	:	depth of specimen (m)
ρ	:	density of specimen (kg/m^3)
E_{dyn}	:	dynamic Young's Modulus
E_{dyn15}	:	dynamic Young's Modulus measured on 15mm thick specimen
E_{dyn36}	:	dynamic Young's Modulus measured on 36mm thick specimen
E_{stat}	:	static Young's Modulus
E_{stat15}	:	static Young's Modulus measured on 15mm thick specimen